Synthesis of Colloidal Magnesium: A Near Room Temperature Store for Hydrogen

Kondo-Francois Aguey-Zinsou*,† and José-Ramón Ares-Fernández‡

Department of Materials, Queen Mary, University of London, London E1 4NS, United Kingdom, and Laboratorio de Materiales de Interés Energético, Universidad Autonoma de Madrid, Cantoblanco 28049, Madrid, Spain

Received October 8, 2007
Revised Manuscript Received November 28, 2007

Metals at the nanoscale have received increased attention because of their unique properties.[1–3] In this respect, the synthesis of magnesium nanomaterials could lead to interesting applications in the field of batteries and hydrogen storage.[4,5] Magnesium hydride (MgH_2) is an attractive hydrogen store because it is abundant and light and can reversibly store 7.6 mass % hydrogen.[6] However, practical applications are limited by sluggish hydrogen kinetics and the high temperatures of the dehydriding reaction (>350 °C, eq 1).[7,8]

$$MgH_2 + 75\ \text{kJ mol}^{-1} \leftrightarrow Mg + H_2 \qquad (1)$$

To overcome these drawbacks, most studies have focused on the modification of magnesium thermodynamic and hydrogen kinetics properties by ball milling magnesium with alloying elements and a catalyst, respectively.[9–12] Despites some breakthroughs, desorption temperatures remain too high for practical applications (~250 °C). The ideal material would release hydrogen at a temperature close to the one of the proton-exchange membrane fuel cell (~85 °C).[13] From a kinetic point of view, the decomposition of MgH_2 is controlled by the nucleation and growth of the α-phase (solid solution of hydrogen) within the β-phase (hydride phase).[14] In this process, the slow diffusion of hydrogen through the β-phase is the regulating step.[15,16] Recent theoretical work also indicates that MgH_2 is less thermodynamically stable as particle diameter decreases below 2 nm.[17,18] Therefore, a significant decrease in MgH_2 particle size should promote the dehydriding reaction. Experimentally, this size effect has not been extensively investigated because of the difficulty in synthesizing nanoparticles of magnesium, which is a highly reactive metal. Mechanical milling of MgH_2 is limited to particle size down to 300 nm,[19] and in most cases with inhomogeneous size distributions, agglomeration,[20] and impurities.[21] Magnesium nanomaterials synthesized by gas phase condensation are also large (50−200 nm) and fully desorb hydrogen at or above 300 °C.[22,23]

To achieve the preparation of small magnesium particles, we have opted for a synthesis by metal salt reduction in the liquid phase, which offers more control over size.[24] Furthermore, because of the low redox potential of magnesium ($E^0_{Mg^{2+}/Mg} = -2.37$ V), the magnesium salt was electrochemically reduced in a nonaqueous aprotic solvent containing a surfactant as electrolyte and nanoparticles stabilizer. By the similar method of sacrificial anodes, Reetz et al. synthesized nanoparticles of Pd and Pt with a narrow size distribution (1.2–5 nm).[25] However, in the present investigation, a stabilizer thermally stable was needed to avoid side reactions during the hydriding/dehydriding cycles. In addition, a stabilizer carrying a weak capping ligand was chosen to avoid strong bonds at the ligand/nanoparticle interface, which may restrict the adsorption of hydrogen. Therefore, tetrabutylammonium bromide (TBA), which is thermally stable up to 170 °C, was used (Supporting Information, Figure S1). Finally, the electrolysis was carried out in THF to prevent the formation of a passivating film at the electrodes surface.[5]

The light gray precipitate obtained at the end of the electrolysis was characterized by TEM. As shown in Figure

* Corresponding author. Fax: 44 20 8981 9804. E-mail: f.aguey@qmul.ac.uk or f.aguey@ucl.ac.uk.
† Queen Mary, University of London.
‡ Universidad Autonoma de Madrid.

(1) Poizot, P.; Laruelle, S.; Grugeon, S.; Dupont, L.; Tarascon, J.-M. *Nature* **2000**, *407*, 496–499.
(2) Rao, C. N. R.; Müller, A.; Cheetham, A. K., *The Chemistry of Nanomaterials: Synthesis, Properties and Applications*; Wiley-VCH Verlag GmbH & Co. KGaA: Weinheim, Germany, 2004.
(3) Rodumer, E. *Chem. Soc. Rev.* **2006**, *35*, 583–592.
(4) Li, W.; Li, C.; C., Z.; Ma, H.; Chen, J. *Angew. Chem., Int. Ed.* **2006**, *45*, 6009.
(5) Lu, Z.; Schechter, A.; Moshkovich, M.; Aurbach, D. J. *Electroanal. Chem.* **1999**, *466*, 203–217.
(6) Schlapbach, L.; Züttel, A. *Nature* **2001**, *414*, 353–358.
(7) Grochala, W.; Edwards, P. P. *Chem. Rev.* **2004**, *104*, 1283–1316.
(8) Bogdanović, B.; Ritter, A.; Spliethoff, B. *Angew. Chem., Int. Ed.* **1990**, *29*, 223–328.
(9) Dehouche, Z.; Goyette, J.; Bose, T. K.; Huot, J.; Schulz, R. *Nano Lett.* **2001**, *1*, 175–178.
(10) Friedrichs, O.; Aguey-Zinsou, F.; Ares Fernández, J. R.; Sánchez-López, J. C.; Justo, A.; Klassen, T.; Bormann, R.; Fernández, A. *Acta Mater.* **2006**, *54*, 105–110.
(11) Zaluska, A.; Zaluski, L.; Ström-Olsen, J. O. *Appl. Phys. A: Mater. Sci. Process.* **2001**, *72*, 157–165.
(12) Tessier, P.; Akiba, E. *J. Alloys Compd.* **1999**, *293–295*, 400–402.
(13) Steele, B. C. H.; Heinzel, A. *Nature* **2001**, *414*, 345–352.
(14) Gerard, N.; Ono, S., *Hydrogen in Intermetallic Compounds II: Surface and Dynamic Properties, Applications: 2*; Springer-Verlag: Weinheim, Germany, 1992.
(15) Bérubé, V.; Radtke, G.; Dresselhaus, M. S.; Chen, G. *Int. J. Energy Res.* **2007**, *31*, 637–663.
(16) Fernández, J. F.; Sánchez, C. R. *J. Alloys Compd.* **2002**, *340*, 189–198.
(17) Cheung, S.; Deng, W.-Q.; van Duin, A. C. T.; Goddard, W. A. *J. Phys. Chem. A* **2005**, *109*, 851–859.
(18) Wagemans, R. W. P.; van Lenthe, J. H.; de Jongh, P. E.; Jos van Dillen, A.; de Jong, K. P. *J. Am. Chem. Soc.* **2005**, *127*, 16675–16680.
(19) Aguey-Zinsou, K.-F.; Ares Fernandez, J. R.; Klassen, T.; Bormann, R. *Int. J. Hydrogen Energy* **2007**, *32*, 2400–2407.
(20) Aguey-Zinsou, K.-F.; Ares Fernandez, J. R.; Klassen, T.; Bormann, R. *Mater. Res. Bull.* **2006**, *41*, 1118–1126.
(21) Ares, J. R.; Aguey-Zinsou, K.-F.; Klassen, T.; Bormann, R. *J. Alloys Compd.* **2007**, *434–435*, 729–733.
(22) Li, W.; Li, C.; Ma, H.; Chen, L. *J. Am. Chem. Soc.* **2007**, *129*, 6710–6711.
(23) Shao, H.; Wang, Y.; Xu, H.; Li, X. *Mater. Sci. Eng., B* **2004**, *110*, 221–226.
(24) Cushing, L. B.; Kolesnichenko, V. L.; O'Connor, C. J. *Chem. Rev.* **2004**, *104*, 3893–3946.
(25) Reetz, M. T.; Winter, M.; Breinbauer, R.; Thurn-Albercht, T.; Vogel, W. *Chem.—Eur. J.* **2001**, *7*, 1084–1094.

10.1021/cm702897f CCC: $40.75
Published on Web 12/27/2007

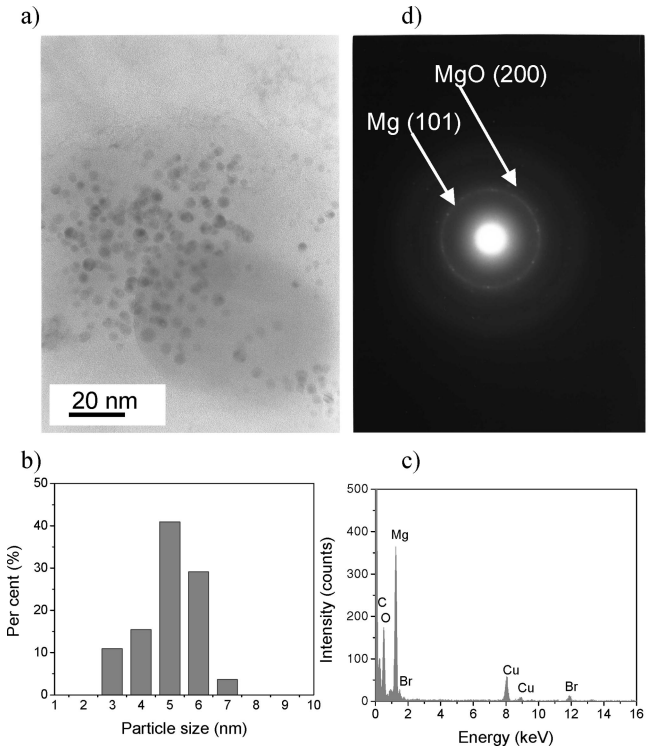

Figure 1. (a) Transmission electron microscopy (TEM) image of the Mg colloid. (b) Mg particle size distribution. (c) Selected-area electron diffraction (SAED) pattern of the Mg nanoparticles. (d) Energy-dispersive X-ray spectroscopy (EDS) of the Mg colloid.

1a, spherical nanoparticles were obtained and their size distribution is very narrow and centered around 5 nm (Figure 1b). Analysis by EDS reveals that the nanoparticles are composed of magnesium (Figure 1c). The precipitate contains some bromide coming from the surfactant. The latter was observed by IR spectroscopy (Supporting Information, Figure S2). SAED pattern reveals diffraction rings indexed to crystalline magnesium and MgO, respectively (Figure 1d). MgO is probably due to a partial oxidation of the magnesium particles during the transfer in air of the colloid to the TEM. The colloid contains 18 mass % Mg according to elemental analysis.

Once hydrided under a hydrogen pressure of 2 MPa at 60 °C, the MgH_2 colloid was characterized by thermal analysis. As presented Figure 2a, the thermogram obtained shows two decomposition steps related to the decomposition of (a) the TBA salt left within the colloidal structure, and (b) the TBA shell stabilizing the Mg core (see the Supporting Information). However, compared to the non-hydrided Mg colloid, the first decomposition starts at a lower temperature of 100 °C and exhibits a higher mass loss of 4.8% instead of 3.3%. In addition, a more intense endothermic peak is observed at 165 °C by DTA (Figure 2b). Analysis of the gases arising from the decomposition of the hydrided colloid reveals that first hydrogen is released from 100 °C, and then hydrogen gas corresponding to the decomposition of TBA appears above 250 °C (Figure 2c). By comparison, the decomposition of the non-hydrided Mg colloid does not show any hydrogen below 250 °C, (Figure 2c). Therefore, the additional mass loss and the more intense endothermic peak at 165 °C are due to the decomposition of MgH_2. According to the thermograms, 1.5 ± 0.2 mass % hydrogen was stored in the

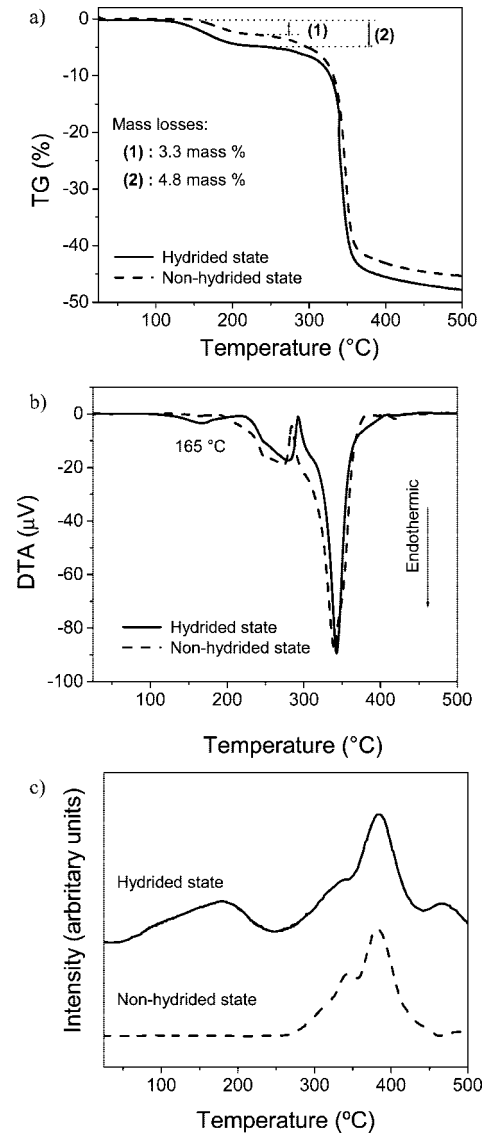

Figure 2. (a) Thermogram (TG) of the Mg colloid after H_2 absorption (hydrided sate) and desorption (non-hydrided state). Mass losses are given ±0.1%. (b) Associated differential thermal analysis (DTA) signals. c) Evolution of H_2 followed by mass spectrometry during the thermal decomposition of the colloids.

colloid. This corresponds to a fully hydrided magnesium containing 7.6 mass % hydrogen.

In isothermal conditions, full dehydriding takes 5.3 h at 85 °C (Figure 3a). According to mass spectrometry measurements, a total amount of 1.34 ± 0.01 mass % hydrogen was desorbed (7.6 mass % H_2 in Mg). This value is close to the theoretical capacity of the colloid, i.e., 1.38 mass %. Because the major problem with MgH_2 is the high temperature required for hydrogen desorption, the result obtained is remarkable. In comparison, MgH_2 nanomaterials with larger sizes (>80 nm) would not desorb hydrogen below 200 °C.[22,23] This demonstrates the importance of size on the dehydriding kinetic of MgH_2.

The rate-limiting step of the reaction was determined by using the classical theory of solid–gas reaction kinetics.[26] As shown Figure 3b, the fraction reacted $F(\alpha)$ exhibits a sigmoidal shape that can be fitted by the rate expression

(26) Mintz, M. H.; Zeiri, Y. *J. Alloys Compd.* **1994**, *216*, 159–175.

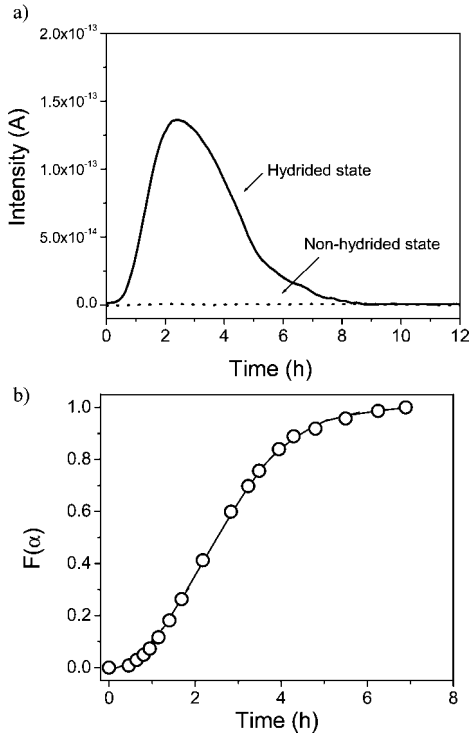

Figure 3. (a) H_2 desorption followed by mass spectrometry for the MgH_2 (hydrided state) and the Mg colloids (non-hydrided state) at 85 °C. No other gases were detected during H_2 desorption. (b) Plot of the dehydrided fraction $F(\alpha)$ as function of time. $F(\alpha)$ corresponds to the amount of MgH_2 converted into Mg and was calculated by integrating the total ion current for H_2 at different times.

$[-\ln(1-F(\alpha))]^{1/2} = kt$ (Supporting Information, Figure S4). Therefore, the rate limiting step of the dehydriding reaction of the MgH_2 colloid is the nucleation and growth of the α-phase.[14] During this process, the growth of the Mg nuclei is controlled by the reaction at the Mg/MgH_2 interface, suggesting that the thermodynamic driving force is finally the only one controlling the reaction. Thus, neither diffusion (due to small diffusion paths) nor surface effects seems restrictive anymore.[26]

According to the Van't Hoff plot of bulk MgH_2, the equilibrium pressure (P_{eq}) below which the dehydriding reaction can take place is 7 Pa at 85 °C.[27] We have observed that the hydriding reaction of the MgH_2 colloid occurs under a hydrogen pressure of 300 Pa at 85 °C. This suggests a substantial increase in P_{eq} compared to bulk MgH_2, i.e., MgH_2 colloid would be less thermodynamically stable. The reduced stability of the Mg nanoparticles could be induced by the stabilizer and/or the high surface to volume atom ratio.[24,28]

In conclusion, surfactant-stabilized magnesium nanoparticles with a diameter of 5 nm, have been successfully prepared by electrochemical synthesis. They exhibit unique hydrogen storage properties, because they can reversibly store ~7.6 mass % hydrogen near room temperature (1.34 mass % by taking into account the surfactant). Although hydrogen cannot be desorbed from bulk MgH_2 below 350 °C, full hydrogen desorption is obtained with colloidal MgH_2 at 85 °C. Our results demonstrate that magnesium hydride properties are size dependent. Investigations to further the understanding of this behavior are in progress.

Acknowledgment. This work was financially supported by the Ramón Y Cajal program (RYC-2005-001054). We thank Dr. F. Bedioui, Prof. C.Sánchez, Prof. J.F Fernandez, and Prof X. Guo for helpful discussions.

Supporting Information Available: Materials and methods; thermal analysis of TBA; infrared spectrum of the Mg colloid; mass spectra corresponding to the gas evolution during the thermal decomposition of TBA and the Mg colloid; fit of the reacted fraction $F(\alpha)$ (PDF). This information is available free of charge via the Internet at http://pubs.acs.org.

CM702897F

(27) Klose, W.; Stuke, V. *Int. J. Hydrogen Energy* **1995**, *20*, 309–316.
(28) Pundt, A. *Adv. Eng. Mater.* **2004**, *6*, 11–21.